THE JOURNAL OF PHYSICAL CHEMISTRY B

 VOLUME 107, NUMBER 20, MAY 22, 2003

LETTERS

Single-Wall Nanostructured Carbon for Methane Storage

Elena Bekyarova,[†] Katsuyuki Murata,[†] Masako Yudasaka,[†] Daisuke Kasuya,[‡] Sumio Iijima,[†,‡,§] Hideki Tanaka,[#] Hirofumi Kahoh,[⊥] and Katsumi Kaneko*[,#,⊥]

Nanotubulities Project, JCORP-JST, c/o NEC Corporation, 34 Miyukigaoka, Tsukuba 305, Japan, Meijo University, 1-501 Shiogamaguchi, Tempaku, Nagoya 468-8502, Japan, NEC Corporation, 34 Miyukigaoka, Tsukuba 305-8501, Japan, Center for Frontier Electronics and Photonics, Chiba University, 1-33 Yayoi, Inage, Chiba 263-8522, Japan, and Department of Chemistry, Faculty of Science, Chiba University, 1-33 Yayoi, Inage, Chiba 263-8522, Japan

Received: December 25, 2002; In Final Form: March 20, 2003

Open single-wall carbon nanohorns (SWNHs) were compressed repeatedly at 50 MPa to generate a nanocarbon material of high bulk density. TEM observations and Raman spectroscopy revealed a significant distortion in the structure of the compressed SWNHs. The obtained nanostructured disordered carbon exhibits a high methane storage capacity, reaching 160 cm^3/cm^3 of nanocarbon at 3.5 MPa and 303 K. Comparison of the experimental results with grand canonical Monte Carlo simulations indicates the importance of the adsorption in the interstitial channels for the high total adsorption capacity of the generated nanostructured carbon.

Introduction

The intriguing properties of nanostructured carbons have stimulated an intensive search for novel structures.[1−4] The fabrication strategies are based on arc-discharge,[1] laser ablation,[5] chemical vapor deposition (CVD),[6] templated synthesis,[3] and high-pressure experiments.[7] Unique possibilities for adsorption application may arise from the ability to exploit the high intrinsic porosity of the lightweight carbon network, which is comprised of single-wall graphitic channels. Theoretical and experimental studies have focused on optimizing the pore structure of carbon materials as promising gas-storage media.[8−13] Recently, open metal-organic frameworks with tunable porous structures,[14] highly microporous coordination polymers,[15] and organic crystals[16] have been studied for their ability to store methane. However, these materials are unlikely to compete with carbon, which has high thermal and chemical stability, in addition to its hydrophobic nature. Here, we show that a carbon nanostructure of randomly oriented small tubular fragments interconnected in a highly porous network can be generated by repeatedly compressing open single-wall carbon nanohorns (SWNHs). The obtained compound exhibits high ability to store methane at almost room temperature: the capacity reaches 160 cm^3/cm^3 of carbon nanohorns at 3.5 MPa and 303 K. The choice of SWNHs as gas-storage media is based on the high purity and specific morphology of the material. Nanohorns, which are formed in a synthetic process without a metal catalyst, exhibit a pure graphitic structure. In contrast to carbon nanotubes, which grow in a triangular lattice with narrow intertubular gaps, nanohorns self-assemble in spherical aggregates, with space between the adjacent nanohorns that is large enough to accommodate small gas molecules. This organization of the nanohorns is beneficial for adsorption utilization, because the gas molecules can be stored in both the cylindrical inner

* Author to whom correspondence should be addressed. E-mail: kaneko@pchem2.s.chiba-u.ac.jp. Fax: 81-43-290-2788.
[†] Nanotubulities Project, JCORP-JST.
[‡] Meijo University.
[§] NEC Corporation.
[#] Center for Frontier Electronics and Photonics, Chiba University.
[⊥] Department of Chemistry, Faculty of Science, Chiba University.

10.1021/jp0278263 CCC: $25.00
Published on Web 04/30/2003

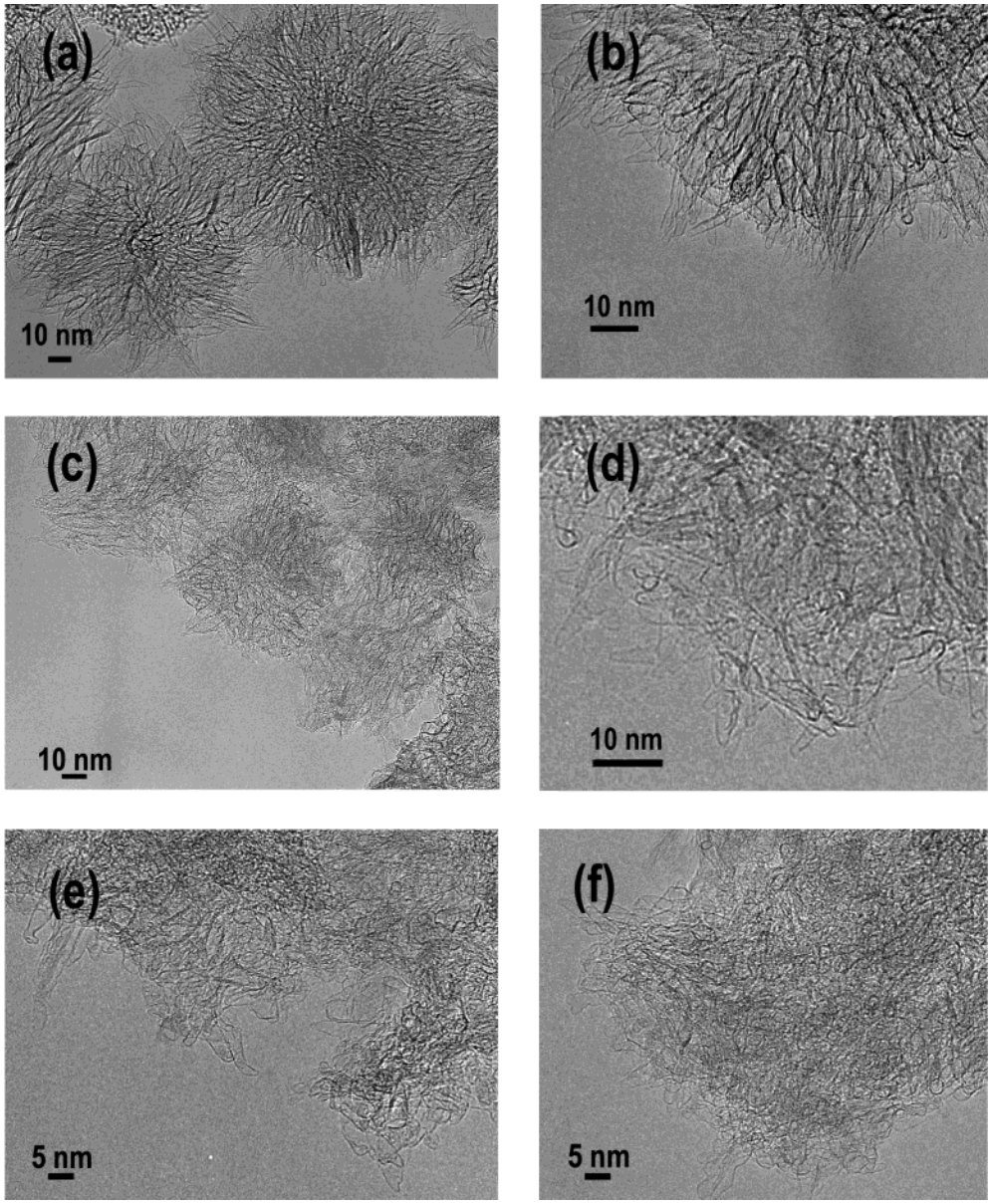

Figure 1. TEM micrographs of single-wall graphitic nanostructures. A low-magnification TEM image of as-grown SWNH (a) shows the typical spherical morphology of the nanoaggregates composed of radially oriented SWNHs with conical tips, as illustrated in a high-magnification micrograph (b). After opening and compression, the structure of the nanohorns undergoes significant changes: most of the aggregates lose their spherical appearance (c), and many individual nanohorns are strongly bent (d). The compressed SWNHs lose their conical tips, generating a network of randomly oriented nanotubule-like particles (e, f).

nanospace and interstitial channels. Apart from this, SWNHs are easy to manufacture with a high yield (∼95%), which makes them increasingly cheap. When a pressure of 50 MPa is applied to SWNHs, the morphology of the spherical nanohorn aggregates does not change substantially, the apparent volume shrinks by a factor of 20, and micropores develop.[17] In attempts to improve the packing density and modify the pore network by further increasing the ratio of narrow pores to wide pores, SWNHs with open nanohorns were subjected to successive cycles of compressing at 50 MPa under vacuum and crushing the pellet. This procedure resulted in unexpected changes of the structure.

Results and Discussion

We prepared SWNHs by laser-ablating graphite without a catalyst at room temperature; the size and morphology of a given aggregate is controlled by the type and pressure of the buffer gas in the chamber.[18,19] *Dahlia*-SWNHs were prepared in argon at 760 Torr. The vaporization of carbon produces graphitic particles with a uniform size of ∼80 nm, composed of SWNHs with a diameter of 2−3 nm (Figure 1a, b). The nanohorns were opened by heating the soot in O_2 at 420 °C for 10 min, followed by overnight treatment in H_2O_2. The black residue was filtered, dried at 60 °C, and heat-treated in argon at 900 °C to remove the oxygen functionalities that were produced during the opening process. The powder was then dispersed in ethanol, dried in air, and mechanically compressed at 50 MPa under vacuum for 10 min. After nine cycles of crushing the pellet and successive compressing, a thin disk was obtained, with a bulk density of 0.97 g/cm^3, as calculated from the weight and geometrical volume. We will refer to the resulting material as compressed SWNHs. Electron microscopy studies revealed significant distortion in the structure of SWNHs after the repetitive compression. The spherical aggregates appear severely deformed

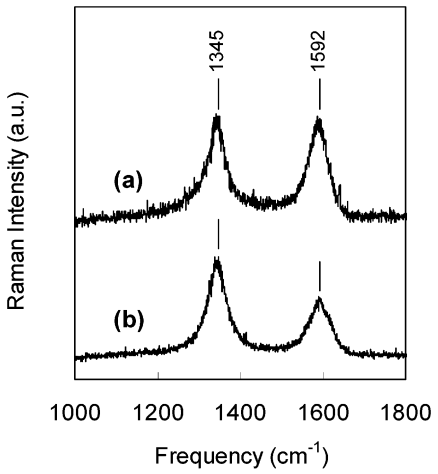

Figure 2. Raman spectra of SWNH samples taken with 488-nm excitation ((a) as-grown SWNHs and (b) compressed SWNHs).

(Figure 1c). Most likely, after the repetitive compression, some of the aggregates coalesced, complicating the TEM observations. Although the individual nanohorns in the as-grown spherical aggregate are radially oriented (Figure 1a, b), the ordered structure inside the aggregates of the compressed SWNHs is greatly disrupted (Figure 1d−f). There are very few remaining typical nanohorn structures. Many of the nanohorn particles have lost their regular shape and appear strongly damaged and without conical tips. The observed nanotubular units have been substantially bent and twisted, generating a network of randomly oriented single-wall carbon nanotubules. It should be noted that a single compression of as-grown SWNHs does not cause significant changes in the nanohorn structure,[17] which is in accordance with the intrinsic high stiffness and strength of the sp^2-bonded carbon material.[20−22] The observed distortion in the structure of the compressed open nanohorns is presumably associated with the presence of many defects in the open nanohorns (as a result of the oxidation process), decreasing the mechanical strength of the graphitic nanohorn units. In addition, the deformation of the nanohorns might be mediated by defects created during the repetitive compression.

The structure changes were also characterized by Raman scattering measurements (Figure 2). The as-grown *dahlia*-SWNH exhibits a spectrum characteristic of SWNHs with a disorder-induced Raman peak (*D*-band) at 1345 cm^{-1} that is almost identical in intensity to the peak centered at ∼1590 cm^{-1} (*G*-band). Lowering the symmetry in the compressed SWNHs gives rise to an increased relative intensity of the *D*-band peak to the *G*-band peak. In addition, the *G*-band peak broadens. The Raman data clearly reflect increased disorder in the structure of SWNHs after compression.

An important question that arises in regard to the gas-storage ability is whether the generated structure is open and whether the channels are accessible for gas molecules. Evidence for the high permeability of the channels was obtained from the measured particle density by high-pressure helium buoyancy. The particle density determined for the compressed SWNHs (2.2 g/cm^3) is similar to the theoretical density of graphite, indicating that the present pores in the graphitic network are open and available for adsorption. The pore structure was further studied by nitrogen adsorption measurements at 77 K. Figure 3 illustrates the nitrogen isotherms of the open nanohorns before and after the compression. Obviously, the porosity undergoes remarkable changes after the compression. In contrast to the micro-mesoporous feature of the sorption isotherm of the uncompressed open SWNHs, exhibiting a continuous increase

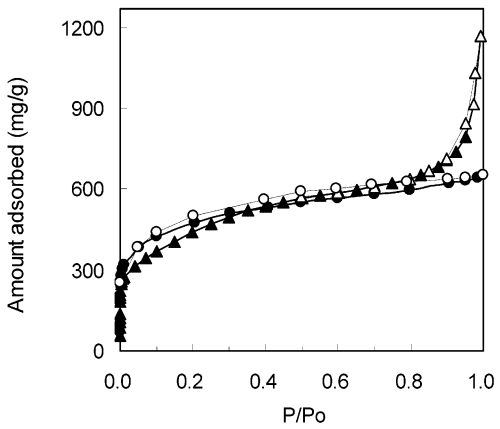

Figure 3. Nitrogen sorption isotherm at 77 K of open SWNHs before compression (triangles) and after compression (circles); closed and open symbols respectively denote adsorption and desorption branches.

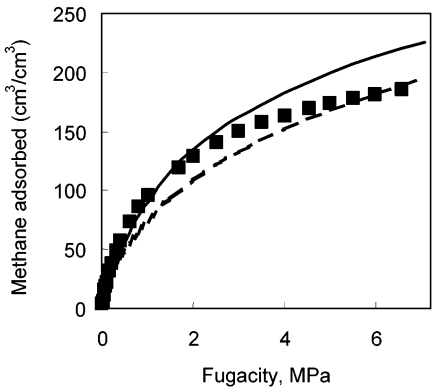

Figure 4. Methane adsorption uptake at 303 K experimentally measured on (■) compressed SWNHs and simulated isotherms in SWNTs organized in (−) square and (− − −) triangular arrays.

of the uptake with the pressure, the isotherm of the compressed open SWNHs is close to type I, which is characteristic for a highly microporous material. The pore-size distribution curves obtained by Barret−Joyner−Halenda (BJH) method (not shown) revealed that, after the compression, most of the pores 3−50 nm in size were suppressed and only a small fraction of mesopores 2−3 nm in size remained. By applying the subtracting pore effect method for the α_s plot,[23] the surface area (*S*) and micropore volume (V_{mi}) of the compressed SWNHs were estimated to be 1097 m^2/g and 0.55 cm^3/g, respectively. The corresponding values for uncompressed SWNHs with open nanohorns are $S = 1030$ m^2/g and $V_{mi} = 0.50$ cm^3/g. The micropore volume increases after the compression. The increase of the value of V_{mi} should be due to the reduction of space between nanohorns of adjacent aggregates brought closely together by the applied mechanical force. A pore structure with predominant micropores and little mesoporosity is ideal for methane storage: at room temperature, methane is adsorbed exclusively in the micropores and capillary condensation in the mesopores does not occur.[9] The pore-structure parameters, coupled with the high bulk density (0.97 g/cm^3), raised an interest in the methane storage ability of the compressed nanohorns. The methane adsorption at 303 K was measured in a gravimetric apparatus that was equipped with a Cahn microbalance. The sample was heated at 423 K under vacuum (10^{-3} kPa) for 2 h before the adsorption measurements. The experimentally measured methane adsorption isotherm of compressed SWNHs is shown in Figure 4. On the basis of volume of methane adsorbed per volume of adsorbent, the methane

uptake reaches 160 cm^3/cm^3 of adsorbent at 303 K and 3.5 MPa, exceeding the U.S. Department of Energy (DOE) target of 150 cm^3/cm^3 of adsorbent that has been set for practical use of storage media. For comparison, the methane adsorption capacity of activated carbon (Maxsorb, $S = 2400$ m^2/g and $V_{mi} = 1.15$ cm^3/g), measured in the same apparatus and under the same conditions as the compressed SWNHs, is 96 cm^3/cm^3 of adsorbent at 303 K and 3.5 MPa. To understand the underlying adsorption mechanism, we compared the experimental data for the compressed SWNHs with simulated methane adsorption in arrays of single-wall carbon nanotubes (SWNTs) with two different geometries: triangular and square arrays. The isotherms were modeled with grand canonical Monte Carlo (GCMC) simulations for open-ended SWNTs with a van der Waals gap (the distance between walls of neighboring tubes) of 0.34 nm. The solid−fluid and fluid−fluid interactions are modeled by the Lennard-Jones potential. The Lennard-Jones parameters are the diameter σ and well depth ϵ/k, where k is the Boltzmann constant. The parameters modeling methane are $\sigma_{ff} = 0.381$ nm and $\epsilon_{ff}/k = 148.12$ K. The graphitic surface was modeled for $\sigma_{ss} = 0.34$ nm, $\epsilon_{ss}/k = 28$ K, and the density of C atoms in the pore wall ($\rho_s = 38.2$ nm^{-2}). The cross parameters for solid−fluid interactions, σ_{sf} and ϵ_{sf}, were calculated by the Lorenz−Berthelot rules. The simulations were performed for a tube diameter of 3.0 nm, as measured from the centers of the C atoms. This diameter is close to that of the (22, 22) nanotube. Although this diameter is much larger than the most abundant type of nanotube observed experimentally, it is similar to the inner diameter of the tubular part of the uncompressed open SWNHs. The high disorder in the structure of the compressed SWNHs, complemented with the presence of two types of channels with different geometry (intratubular and interstitial channels), hampers the precise evaluation of the tubular pore size in the compressed SWNHs. Assuming, to a first approximation, a cylindrical model for the channels, an average size of 2.3 nm was calculated from the nitrogen adsorption data, corresponding to a tube diameter of 2.7 nm, as measured from the centers of the C atoms. The results of our simulations are plotted in Figure 4, along with the experimental data. We observe good agreement between the simulations and the experiment. At low pressures, the compressed SWNHs exhibit an uptake of methane that is comparable with the SWNT square array. Because of the significant contribution of the adsorption in the interstitial channels, more methane is stored in the tubes arranged in a square array. At pressures >4 MPa, the uptake approaches the simulated adsorption isotherm for tubes arranged in a triangular array. The simulations indicate the importance of the tube array configuration for the storage capacity. Consequently, optimizing the tube diameter and the space between adjacent nanotubular units holds potential for further progress in the design of porous carbon for methane storage. The experimentally observed high uptake of methane in the compressed SWNHs is attributed to the ability of the generated carbon nanostructure to accommodate gas molecules in the interstitial nanopores, in addition to the internal nanotubular space.

The mechanical properties of the obtained pellet were not studied. The disk does not disintegrate easily during handling; however, it can be ground in an agate mortar. Additional studies of the mechanical properties would show whether further processing is necessary for enhancement of the pellet strength.

Conclusion

Our results are the first report on extremely high methane adsorption in single-wall carbon nanoporous rigid structures. We anticipate that single-wall carbon nanomaterials with disordered structure could find application as storage media for methane and other supercritical gases. Taking control over the generation process will allow tuning of the nanospace between the nearest tubes, which holds potential for further exploration, and carbon nanomaterials with even higher storage capacity may emerge. Nearly space-filling fractal networks of disordered nanocarbon derived from activated carbon were recently reported to hold promise for gas storage.[24] Addressing the issue of methane storage per volumetric base, the bulk density of the material emerges as an important issue, along with the optimal porosity. The obtained single-wall-structured carbon offers several advantages over other existing carbon nanomaterials. Its pore structure is constructed entirely of single-wall graphene channels. In addition, the interconnection of intricately disordered small nanotubular units is beneficial for fabrication of a densely packed nanostructure, which maintains a high porosity upon compression.

Acknowledgment. E.B. acknowledges a STA grant from JISTEC.

References and Notes

(1) Iijima, S. *Nature (London)* **1991**, *354*, 56.
(2) Ugarte, D. *Nature (London)* **1992**, *359*, 707.
(3) Joo, S. H.; Choi, S. J.; Oh, I.; Kwak, J.; Liu, Z.; Terasaki, O.; Ryoo, R. *Nature (London)* **2001**, *412*, 169.
(4) Yoo, C. S.; Nellis, W. J.; Sattler, M. L.; Musket, R. G. *Appl. Phys. Lett*. **1992**, *61*, 273.
(5) Thess, A.; Lee, R.; Nikolaev, P.; Dai, H.; Petit, P.; Robert, J.; Xu, C.; Lee, Y. H.; Kim, S. G.; Rinzler, A. G.; Colbert, D. T.; Scuseria, G. E.; Tománek, D.; Fischer, J. E.; Smalley, R. E. *Science* **1996**, *273*, 483.
(6) Ren, Z. F.; Huang, Z. P.; Xu, J. W.; Wang, J. H.; Bush, P.; Siegal, M. P.; Provencio, P. N. *Science* **1998**, *282*, 1105.
(7) McMillan, P. F. *Nat. Mater*. **2002**, *1*, 19.
(8) Kaneko, K.; Murata, K.; Shimizu, K.; Camara, S.; Suzuki, T. *Langmuir* **1993**, *9*, 1165.
(9) Menon, V. C.; Komarneni, S. *J. Porous Mater*. **1998**, *5*, 43.
(10) Matranga, K. R.; Myers, A. L.; Glandt, E. D. *Chem. Eng. Sci.* **1992**, *47*, 1569.
(11) Cracknell, R. F.; Gordon, P.; Gubbins, K. E. *J. Phys. Chem*. **1993**, *97*, 494.
(12) Tan, Z.; Gubbins, K. E. *J. Phys. Chem.* **1990**, *94*, 6061.
(13) Tanaka, H.; El-Merraoui, M.; Steele, W. A.; Kaneko, K. *Chem. Phys. Lett.* **2002**, *352*, 334.
(14) Eddaoudi, M.; Kim, J.; Rosi, N.; Vodak, D.; Wachter, J.; O'Keeffe, M.; Yaghi, O. M. *Science* **2002**, *295*, 469.
(15) Noro, S.; Kitagawa, S.; Kondo, M.; Seki, K. *Angew. Chem., Int. Ed.* **2000**, *39*, 2081.
(16) Atwood, J. L.; Barbour, L. J.; Jerga, A. *Science* **2002**, *296*, 2367.
(17) Bekyarova, E.; Kaneko, K.; Yudasaka, M.; Murata, K.; Kasuya, D.; Iijima, S. *Adv. Mater.* **2002**, *14*, 973.
(18) Iijima, S.; Yudasaka, M.; Yamada, R.; Bandow, S.; Suenaga, K.; Kokai, F.; Takahashi, K. *Chem. Phys. Lett.* **1999**, *309*, 165.
(19) Kasuya, D.; Yudasaka, M.; Takahashi, K.; Kokai, F.; Iijima, S. *J. Phys. Chem. B* **2002**, *106*, 4947.
(20) Salvetat, J. P.; Bonard, J. M.; Thomson, N. H.; Kulik, A. J.; Forro, L.; Benoit, W.; Zuppiroli, L. *Appl. Phys. A* **1999**, *69*, 255.
(21) Tang, J.; Quin, L. C.; Sasaki, T.; Yudasaka, M.; Matsushita, A.; Iijima, S. *Phys. Rev. Lett*. **2000**, *85*, 1887.
(22) Treacy, M. M. J.; Ebbesen, T. W.; Gibson, J. M. *Nature (London)* **1996**, *381*, 678.
(23) Setoyama, N.; Suzuki, T.; Kaneko, K. *Carbon* **1998**, *36*, 1459.
(24) Pfeifer, P.; Ehrburger-Dolle, F.; Rieker, T. P.; Gonzalez, M. T.; Hoffman, W. P.; Molina-Sabio, M.; Rodriguez-Reinoso, F.; Schmidt, P. W.; Voss, D. J. *Phys. Rev. Lett*. **2002**, *88*, 115502.